buildings

MDPI

Article

Photocatalytic Activity and Mechanical Properties of Cement Slurries Containing Titanium Dioxide

Yasmine Jabali [1], Joseph Assaad [1,*] and Georges Aouad [2,3]

[1] Department of Civil and Environmental Engineering, University of Balamand, Al Koura, Tripoli P.O. Box 100, Lebanon; yasmine.jabaly@balamand.edu.lb
[2] Centre for Materials and Processes, IMT Nord Europe, Institut Mines-Télécom, F-59000 Lille, France
[3] 4515-LGCgE–Laboratoire de Génie Civil et géoEnvironnement, Institut Mines-Télécom, University Lille, University Artois, F-59000 Lille, France
* Correspondence: joseph.assaad@balamand.edu.lb

Abstract: The effect of titanium dioxide (TiO_2) on the mechanical properties of cement slurries including their benefits on air purification and abatement of pollutants is not well documented. Cementitious-based slurries are typically applied in thin layers as decorative coatings for existing facades, protection against an ingress of aggressive ions, or rainproof covers to minimize water penetration. Different parameters including the TiO_2 concentration, dispersion time during batching, and applied thickness on top of existing mortar blocks are investigated in this paper. Tested properties included the flow, colorimetry, compressive/flexural strengths, bond to existing substrates, water absorption, and photocatalytic activity evaluated using an ISO 22197-1:2007 reactor. The results showed that the mechanical properties remarkably improved with TiO_2 additions, up to 8% of the cement mass. This was attributed to two concomitant phenomena including a micro-filler effect that enhances the packing density and nucleation sites to promote strength development. The removal of nitrogen oxides from the atmosphere reached 92% when the TiO_2 was added at a rate of 5% of the cement mass. Such data can be of particular interest to consultants and environmental activists searching for innovative materials capable of maintaining better ambient air quality in urban and modern cities.

Keywords: cement slurry; titanium dioxide; NOx removal; photocatalytic activity; mechanical properties

check for updates

Citation: Jabali, Y.; Assaad, J.; Aouad, G. Photocatalytic Activity and Mechanical Properties of Cement Slurries Containing Titanium Dioxide. *Buildings* **2023**, *13*, 1046. https://doi.org/10.3390/buildings13041046

Academic Editor: Denny Coffetti

Received: 31 March 2023
Revised: 11 April 2023
Accepted: 14 April 2023
Published: 17 April 2023

1. Introduction

Environmental pollution including the quality of ambient air is adversely affected by modernization and urbanization growth, raising serious global concerns for the human society [1,2]. Mobile sources such as motor vehicles, airplanes, and trains, and stationary sources such as industries and power plants are the main contributors to air pollution, causing the release of air pollutants [3,4]. According to the National Ambient Air Quality Standards (ANAAQS), nitrogen oxides (NOx) are among the most dangerous air pollutants that threaten the ecosystem and human health [5]. The NOx gases participate in the formation of acid rain and photochemical smog [5], and are linked to respiratory illnesses that cause breathing problems, eye irritation, chronically reduced lung function, and loss of appetite [6]. High NOx levels can also damage vegetation and increase the susceptibility to disease and frost attack.

In the building industry, numerous researchers considered embedding titanium dioxide (TiO_2) in cementitious materials applied to external facades and surfaces exposed to sunlight in urban cities [7,8]. Portland cement has long been used as a supporting medium for TiO_2 nanoparticles because of its effective binding ability that generates photocatalytic reactions to protect and self-clean concrete structures [1,9–12]. The photocatalytic process requires the presence of a natural energy source such as solar radiation. Under sunlight irradiation, photons that have energies equal to or higher than the TiO_2 bandgap are absorbed by the photocatalyst. The latter will result in the formation of an energy-rich electron-hole pair (e–h+) that generates photocatalytic oxidation and reduced reactions. The highly reactive superoxide radical-anions (O_2^-) and hydroxyl radicals (•OH) are expected to form on the surface of TiO_2 nanoparticles, which ultimately carry out the neutralization of organic and inorganic contaminants in addition to micro-organisms adsorbed on the surface [13]. It is a continuous process where the TiO_2 has an indefinite photocatalytic activity [14,15]. Li et al. (2016) reported that photocatalytic cement possesses a self-cleaning ability that reduces the discoloration and biological colonization of surfaces, thus offering an eco-friendly approach to solving various environmental problems such as air pollution in urban cities [16].

Numerous standardized experimental methodologies such as the ISO [17] and JIS tests [18] could be used to evaluate the photocatalytic efficiency in the abatement of pollutants. Nevertheless, the recent literature showed that the test results are highly affected by the cementitious materials characteristics including the process parameters and environmental parameters. The materials characteristics are related to the cement matrix pore structure, additive type, cement surface roughness, and mixing/dispersion techniques of TiO_2 particles in the cement matrix. These factors can significantly affect the consistency and photocatalytic performance of the developed product [19,20]. For instance, white cement revealed higher photocatalytic efficiency when compared to grey-colored cement [1]. Moreover, the dispersion of TiO_2 nanoparticles using polycarboxylate-based superplasticizers showed higher NOx removal, compared with other water dispersion admixtures [6]. On the other hand, environmental parameters are those related to the wavelength of UV light, characteristics and concentration of the pollutants, and relative humidity [21]. In this context, it was reported that higher photocatalytic activity could be achieved with a more intense UV source [22]. Martinez et al. (2011) found that relative humidity has a negligible effect on the photo-degradation activity associated with increased NOx emissions [23].

In a recent article by Daniyal et al. (2019), the effect of 1%, 3%, and 5% nano-TiO_2 (NT) content on the fresh, mechanical, and corrosion properties of cementitious mixtures were studied under various exposure conditions such as tap water, brackish water, and acidic solution [24]. Numerous tests were carried out such as setting time, compressive strength, scanning electron microscope (SEM), energy dispersive X-ray (EDX), X-ray diffraction, (XRD), and potentio-dynamic polarization. The setting time demonstrated that the NT acts as an accelerator, while their addition improved the mortar's 28-day compressive strength. The SEM and XRD analysis showed that NT strengthened the microstructure and enhanced the quantity of the desired hydration products. The NT-admixed mortar's 360-day compressive strengths were higher than those of the control mortar subjected to tap water, brine water, or acidic solution. In all exposure conditions, it was found that the increase in the NT dosage enhanced the effectiveness towards corrosion inhibition.

Lee et al. (2021) investigated the environmental photocatalytic performance of concrete blocks containing Nano SiO_2-TiO_2 (NST) additive with SiO_2 acting as a coat and support for TiO_2 [25]. The small-scale and full-scale chamber laboratory tests showed reduced NO efficiency reaching a maximum of 59.1% depending on the UV intensity for concrete blocks containing 4% NST. The reduced efficiencies for NO and SO_2 at 564 W/m^2 of solar radiation were 22.3% and 14.4%, respectively, as per the full-scale testing results. Lapidus et al. (2022) studied the surface sensitization of TiO_2 using graphene oxide to improve the photocatalytic effectiveness [26]. The ideal concentration of TiO_2 and cellulosic materials was found to hover between 0.8–1.1% and 0.4–0.8%, respectively. When investigating the structure of composites, it was observed the TiO_2 was adsorbed onto the surface of swollen cellulose fibers and remained there. The approach of surface sensitizing TiO_2 with graphene oxide additions was proven to be efficient.

Diamanti et al. (2021) investigated the performance characterization of aging materials using several self-cleaning cement-based materials based on photocatalytic principles containing TiO_2 [27]. The materials were exposed to UV light, rain, freeze–thaw cycles, and fluctuations in temperature. The goal of the accelerated aging tests which included a variety of commercial materials was to characterize the photocatalytic activity and self-cleaning capability as a function of time. The experimental campaign indicated the genuine self-cleaning behavior of these materials in their freshly manufactured state, yet with the negative impact of aging on the material performance. Jimenez-Relinque and Castellote (2019) evaluated the photocatalytic activity of TiO_2 building materials, emulsion coatings, and cement-based samples using ink made of a redox dye, nitro blue tetrazolium (NBT), and a sacrificial electron donor, glycerol [28]. Digital photography, a portable colorimetric spectrophotometer, and UV spectroscopy were utilized to track how the ink's color changes as the photocatalytic process develops. Using the ISO 22197-1:2007 test, it was possible to establish a linear dependence between the two sets of findings by comparing the relative rate of NBT ink reduction with the rate of oxidative NOx elimination.

In addition to the photocatalytic activity, TiO_2 particles can participate in the cement hydration process to accelerate the setting times and yield higher strengths at early and late ages. Yang et al. (2017) reported that the beneficial TiO_2 effects can be attributed to a micro-filler effect that enhances the matrix denseness and refines its microstructure [15]. Chen and Poon (2009) showed that the nanoparticles could work as nucleation sites to promote strength development and convert a greater volume of calcium hydroxide into C-S-H gels [1]. Folli et al. (2012) reported that improved strength can be related to higher packing the density of the binder phase that enhances the interfacial transition zones with the sand and coarse aggregate particles [29]. Similar conclusions were made by Assaad (2016) and Assaad et al. (2020) when considering the use of TiO_2 in cementitious overlays and waste latex paints (WLPs) during the production of concrete mixtures intended for sidewalk, stamped, or road barrier applications [30,31]. Besides the environmental benefits, the WLPs conferred increased the concrete flexural and bond strengths, which was attributed to a higher tensile strength of latex films and bond improvement at the hydrated paste–aggregate interfacial transition zone due to TiO_2 particles. The WLP contained 45% acrylic co-polymers, 15% TiO_2, and 15% calcium carbonate extender.

2. Context and Scope of This Study

Cement slurries are composite suspensions made of cement and pozzolans mixed with water and a selected combination of chemical admixtures [32,33]. Their use in the building industry considerably increased in recent years to cover a wide range of architectural to structural applications such as decorative coatings for existing facades and concrete blocks, protective layers against an ingress of aggressive chloride and sulphate ions, repair of damaged surfaces and fissures, and rainproof covers to prevent water penetration [34,35]. The slurries are typically applied in a thin layer using paintbrushes or masonry trowels.

To date, the effect of TiO_2-modified cement slurries on air purification and abatement of pollutants is still not well investigated. This paper is part of a comprehensive project that assesses the efficiency of TiO_2-modified slurries to mitigate the NOx levels in the ambient atmosphere. Its first phase aims at assessing the effect of TiO_2 on workability and mechanical properties, while the second phase evaluates the photocatalytic activity using a reactor developed as per the ISO 22197-1:2007 specification [17]. Different parameters including the TiO_2 concentration, dispersion time during batching, and applied thickness on top of existing mortar blocks are investigated. The combined effect of TiO_2 with other chemical admixtures such as superplasticizer and polymeric latexes used in cement slurries, along with the validation of test results using large-scale photocatalytic mock-ups are presented in a follow-up paper. Such data can be of particular interest to civil engineers, contractors, and environmental activists that search for innovative and sustainable materials that maintain the higher ambient air quality in urban and modern cities.

3. Materials and Methods

3.1. Materials

Commercially available limestone-based, grey-colored Portland cement conforming to BS EN 197/1 was used in this study; the clinker and limestone contents were about

65% and 35%, respectively. The chemical composition of the cement including the CaO, SiO_2, Al_2O_3, Fe_2O_3, and MgO were 68.5%, 21.8%, 4.15%, 0.27%, and 1.18%, respectively. Its specific gravity, Blaine fineness, loss on ignition, and 28-days heat of hydration are 3.15, 3890 cm^2/g, 0.55%, and 288 J/g, respectively. The gradation of siliceous sand complied with the ASTM C33 specification; its specific gravity, fineness modulus, and absorption rate were 2.65, 3.14, and 0.78%, respectively. The sand particles passing a sieve opening of 4.75, 2.36, 1.18, 0.6, and 0.3 mm were 100%, 87.7%, 69.8%, 42.5%, 13.5%, and 3.4%, respectively.

The white-colored TiO_2 is rutile-based and manufactured by the chloride process with a specific gravity of 4.1. The approximate cost of commercially available TiO_2 powder varies between 2.5 to 3.5 USD/kg. Figure 1 shows the scanning electron microscopy (SEM) image for the TiO_2 powder, along with its particle size distribution determined using a laser diffraction analyzer. As shown, the TiO_2 possesses a spherical shape with a fineness remarkably smaller to the cement, which shifted the gradation curve towards much smaller particle sizes. The maximum TiO_2 particle size is less than 2 μm; the resulting median particle size (d_{50}) varied from 0.21 to 26.3 μm for the TiO_2 and cement materials, respectively.

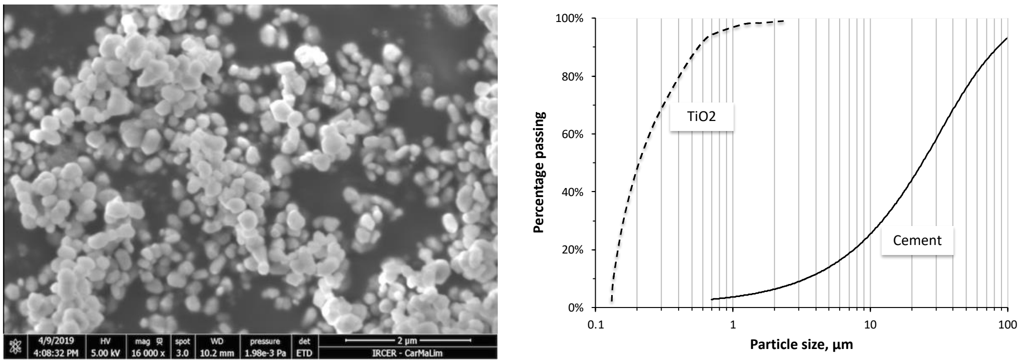

Figure 1. Morphology (**left**) and particle size distribution (**right**) of TiO_2 particles.

3.2. Cement Slurry Proportions

The slurry mixtures used throughout this work had a fixed water-to-cement ratio (w/c) of 0.4. This w/c was selected following preliminary tests to ensure a flowable mixture that can be applied using a paintbrush, yet with adequate homogeneity to secure minimum bleeding and/or segregation. No chemical admixtures were used to avoid interferences on colorimeter and NOx measurements. The flow of the control slurry made without TiO_2 is 220 ± 15 mm, when determined using the mini-slump cone as per ASTM C230.

The TiO_2 particles were introduced at different incremental substitution rates varying from 2% to 10% of the cement content, on a mass basis (this would induce an increase in the cost of the cement slurry mixture varying from 0.3 to 1 USD/kg). Mixing was made using a high-shear laboratory mixer rotating at 250 rpm; the mixing sequence consisted of homogenizing the water and cement for about 2 min until the blend is uniform. After a 30 s rest period, the TiO_2 is introduced, and mixing is resumed for 2 or 8 additional min to determine the effect of dispersion time on the photocatalytic activity. The ambient temperature and relative humidity (RH) during testing remained within 23 ± 3 °C and 55 ± 5%, respectively.

3.3. Testing Procedures

3.3.1. Flowability and Density

The flowability was determined right after mixing using a mini-slump cone having a top diameter, bottom diameter, and height of 70, 100, and 50 mm, respectively. The flow was reported as the average diameter of the slurry after spreading on the flow table. A calibrated volume of 0.75 L was used for measuring the fresh density, while the hardened density was determined after 28 days by weighing the hardened 50 mm cubic specimens. All the slurries were filled in one layer flush with the top of the container, and gently rodded to ensure proper filling. The flow, density, and hardened properties of the tested slurries are summarized in Table 1.

Table 1. Flow, density, and hardened properties of cement slurries.

TiO_2, %	Flow, mm	Density (Fresh), kg/m^3	Density (Hardened), kg/m^3	f′c, MPa	fr, MPa	Pull-Off Bond, MPa	W_{abs}, $mm/min^{0.5}$
0	220	1950	1920	46.2	7.4	2.35	0.414
2	220	1975	1935	47.3	7.8	2.41	0.374
4	215	1970	1960	49	8.8	3.02	0.311
6	195	1990	2005	54.3	9.9	3.5	0.247
8	180	2005	2000	55.2	10.5	3.63	0.174
10	165	2020	2015	53.7	10.7	3.78	0.235

3.3.2. Colorimetry

A portable colorimeter was used to determine the CIE (Commission Internationale d'Eclairage) color coordinates including L, a, and b. In this coloring system, the L-value represents the lightness varying from 0 (black) to 100 (white), a-value represents the chromatic intense of magenta/red (+127) and green (−128), while the b-value represents the chromatic intense of yellow (+127) and blue (−128) [36,37]. The prismatic-shaped specimens were oven-dried at 50 ± 5 °C to eliminate surface moisture prior to color testing. The colorimetry indices for hardened slurries are presented in Table 2; the deviation in color (i.e., Δ(E) index) due to TiO_2 additions from the control slurry was quantified using the following Equation (1):

$$\Delta(E) = \sqrt{(L_{Control} - L)^2 + (a_{Control} - a)^2 + (b_{Control} - b)^2} \quad (1)$$

Table 2. Effect of TiO_2 additions on color characteristics.

TiO_2 Content, %	L-Value	a-Value	b-Value	Δ(E)
0	58.3	2.6	14.5	-
2	63.4	2.8	16.6	5.5
4	68	2.5	18	10.3
6	73.7	2.4	21.2	16.8
8	77	1.9	20.8	19.8
10	78.8	2.1	22.7	22.1

3.3.3. Flexural and Compressive Strengths

The batched slurries were cast in one layer in 40 × 40 × 160 mm prisms, which then were demolded after 24 h. Curing was made in lime saturated water for 7 days, and then in ambient air conditions of 23 ± 3 °C and RH of 55 ± 5% until the age of 28 days. Testing was performed as per BS EN 196/1 Test Method (2016) [38].

3.3.4. Bond Strength

The pull-off bond of the cement slurry to the existing concrete substrate was evaluated as per the EN 1542 Test Method (EN 1542, 1999) [39]. The unreinforced substrates were prepared using 50 mm thick concrete slabs having a compressive strength of about 30 ± 4 MPa. The top concrete surfaces were thoroughly roughened using a steel-wire brush to remove the thin laitance layer and free particles. For application, the cement slurries were filled in the mini-slump cone placed at the substrate center, then lifted to allow spreading. Before pull-off testing after 28 days, the slabs were core-drilled at different locations; the diameter of each core was 50 mm extended to a depth of around 25 mm (Figure 2). The pull-head steel plates were glued using epoxy resins on the test areas, and tensile load was applied until failure at a rate of 0.1 MPa/s. The fracture patterns (i.e., at the interface between the slurry and substrate or within the overlay itself) are noted [40,41].

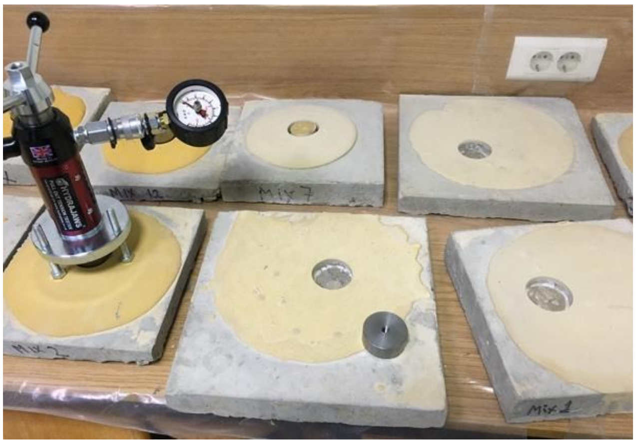

Figure 2. Photo showing the pull-off bond testing set-up.

3.3.5. Water Absorption

The ASTM C1585 (2013) test method was used to determine the sorptivity (or water absorption) of the tested slurries [42]. Prior to testing, the 28-days-aged specimens were oven-dried to a constant mass for 24 h. After being left to cool down to room temperature, the 50 × 50 mm^2 cubes were immersed 2 ± 1 mm in water, and the mass increase due to water absorption was recorded. The rate of water absorption is calculated from the change in mass over time divided by the mortar's cross-section, and multiplied by the water density.

3.3.6. UV Reactor and NOx Measurements

To assess the efficiency of TiO_2-modified slurries on NOx removal, a photocatalytic reactor conforming to ISO 22197-1:2007 and JIS R1701-1 [17,18] was developed. Its main components include a photoreactor cell composed of a 4L cylindrical Plexiglas container with an effective area of 15000 cm^2 equipped with two UV-A fluorescent lamps of 18 W having a peak intensity of 345 nm to provide the UV irradiation (Figure 3). The gas system is composed of a combination of zero air and nitric oxide (NO), a chemiluminescent NOx analyzer was used to measure the resulting concentration of NO inside the reactor, and a thermometer and humidity sensor were inserted inside the reactor. The reactor is entirely sealed and frequently tested for possible leakages. All photocatalytic experiments were carried out at constant environmental conditions (i.e., temperature of 25 °C and RH of 50%).

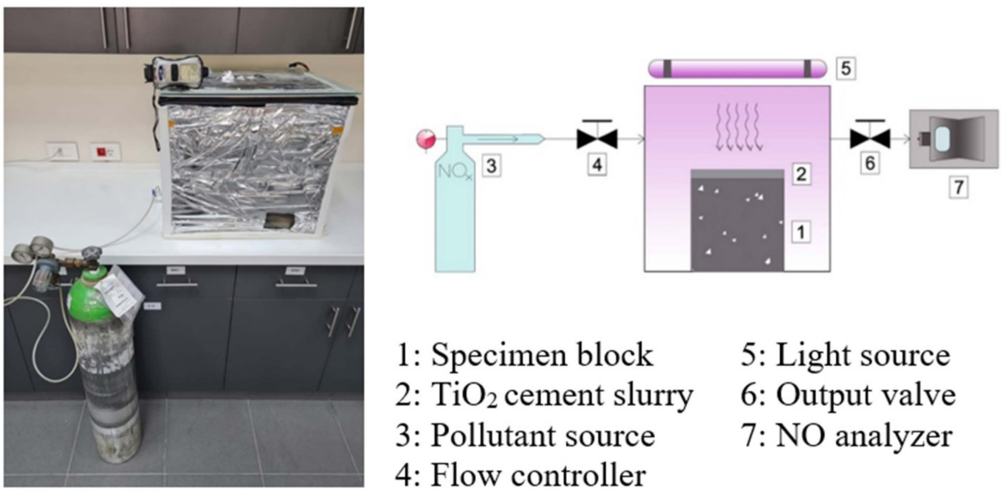

Figure 3. Schematic illustration of the photocatalytic test setup.

The hardened mortar blocks used as a substrate for the slurry application were made of 1-to-3 parts of cement to sand, with a w/c of 0.5. The blocks had $50 \times 50 \times 50$ mm^3 dimensions. The cement slurries were applied using a paintbrush at two thicknesses of 1 and 3 mm, to assess whether the layer thickness would contribute to reducing the NOx measurements. The composite specimens (i.e., mortar block and applied cement slurry) were placed in a plastic bag and allowed to cure for 28 days. Prior to testing, the uncoated sides of the mortar blocks (i.e., five sides) were covered using sealing films to ensure that only the top surface where the photocatalytic cement slurry is applied becomes exposed to UV light. In total, twelve combinations of cement slurries were tested; the TiO_2 contents were 2.5%, 5%, and 10% by mass of cement, and for each content, two different coating thicknesses (1 and 3 mm) and two different dispersion durations (2 and 8 min) were employed.

For testing, the NO gas concentration was adjusted to a value of 20 ± 0.5 ppm, a value commonly considered as a threshold rate for the presence of pollutants found in ambient air [17,18]. After placing the specimen in the reactor, the NO gas stream was switched on and the system was left to stabilize for 5 min in the dark to reach a constant NO concentration. Subsequently, the UV light was switched on and the irradiation continued for 60 min. Additional blank measurements were conducted for the emptied reactor to ensure the absence of possible leakage and interference for the reactor itself. The photocatalytic activity was measured via the percentage of the variation between the NOx initial (C_{in}) and NOx outflow (C_{out}) concentrations (Equation (2)). The percentage of NOx removal was deducted from the below expression, knowing that the gas flow rate and exposed surface area of all samples remained constant in all experiments. The percent of NOx removal is computed using the following expression, and summarized in Table 3.

$$\text{NOx removal, } \% = \left(1 - \frac{C_{out}}{C_{in}}\right) \times 100 \quad (2)$$

Table 3. NOx properties for tested cement slurries.

	TiO_2, % of Cement	Mixing time, min	Thickness, mm	NOx after Stabilization, ppm	NOx Removal, %
2.5%TiO_2-2 min-1 mm	2.5	2	1	10.8	46.0
2.5%TiO_2-2 min-3 mm	2.5	2	3	13.6	32.0
2.5%TiO_2-8 min-1 mm	2.5	8	1	10.8	46.0
2.5%TiO_2-8 min-3 mm	2.5	8	3	12.0	40.0
5%TiO_2-2 min-1 mm	5	2	1	2.1	89.5
5%TiO_2-2 min-3 mm	5	2	3	2.5	87.5
5%TiO_2-8 min-1 mm	5	8	1	1.6	92.0
5%TiO_2-8 min-3 mm	5	8	3	2.2	89.0
10%TiO_2-2 min-1 mm	10	2	1	7.2	64.0
10%TiO_2-2 min-3 mm	10	2	3	8.5	57.5
10%TiO_2-8 min-1 mm	10	8	1	6.6	67.0
10%TiO_2-8 min-3 mm	10	8	3	8.1	59.5

4. Results and Discussion

4.1. Effect on Flow and Density

The effect of TiO_2 on the flow variations of cement slurries is shown in Figure 4; the fresh density of tested mixtures is also given. Clearly, the flow is marginally affected up to 4% additions as the resulting values varied within the repeatability of testing (i.e., within 220 ± 15 mm), which thereafter gradually curtailed at higher rates. Hence, the flow dropped to 195, 180, and 165 mm at TiO_2 rates of 6%, 8%, and 10%, respectively. As shown in the particle size distribution given in Figure 1, the TiO_2 particles are considerably finer than the cement, which are believed to increase the inter-particle links within the suspension [30,31]. Earlier studies have shown that the incorporation of fine particles could increase the packing density and internal friction, which hinders the ease of flow for the given water content [43,44]. Practically, this reflects that the addition of TiO_2 in cement slurries would necessitate the use of superplasticizers to maintain the same flowability and prevent altering their ease of spreading on the substrates.

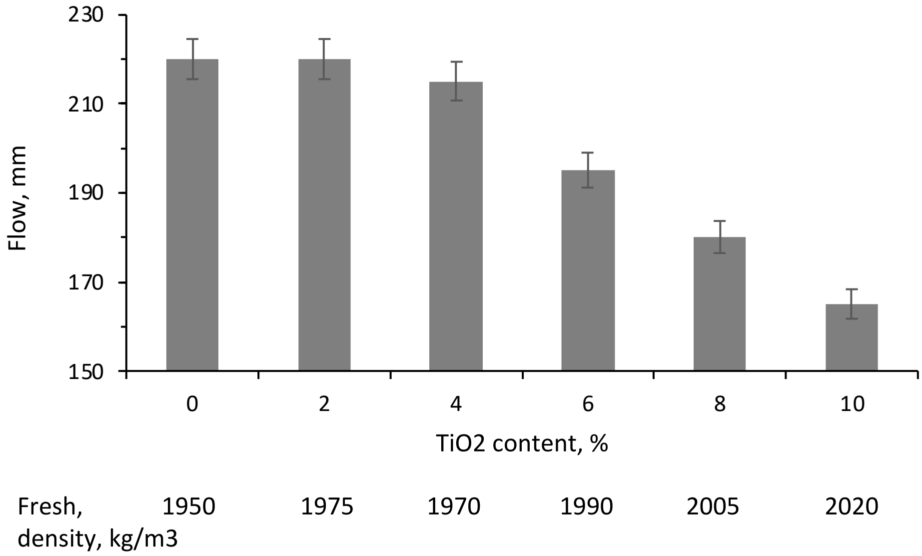

Figure 4. Effect of TiO_2 on flow and density (i.e., fresh) of cement slurries.

It is worth noting that the density (whether fresh or hardened) of mixtures gradually increased with TiO_2 additions; this varied from 1950 kg/m^3 for the control mix to 1970, 2005, and 2020 kg/m^3 for those containing 4%, 8%, and 10%, respectively. This can obviously be attributed to the higher TiO_2 specific gravity (i.e., 4.1 vs. 3.15 for the cement) that could increase the mass of specimens for the given volume.

4.2. Effect on Color Characteristics of the Hardened Slurry

As expected, the specimen's lightness magnitude (i.e., L-value) increased with TiO_2, given the white-colored nature of such pigment additions that are bound onto the cement particles to change its surface color properties. Hence, the L-value varied from 58.3 for the control mix to 68, 73.7, and 78.8 for the mixtures prepared with 4%, 8%, and 10% TiO_2, respectively (Figure 5). The corresponding a-value slightly changed from 2.6 to 2.5, 1.9, and 2.1, respectively, reflecting that the chromatic intensity of magenta/red is marginally affected by the TiO_2. The b-value that reflects the chromatic intense of yellow varied from 14.5 to 18, 20.8, and 22.7, respectively.

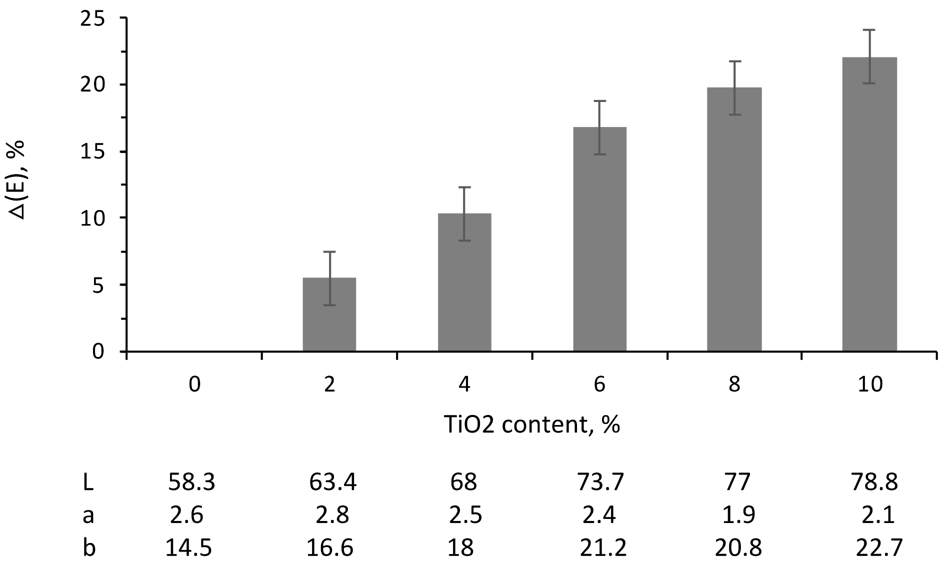

Figure 5. Effect of TiO_2 additions on colorimetry measurements.

As shown in Figure 5, the Δ(E) values gradually increased with TiO_2 additions; these varied from 5.52 to 16.8 and 22.08 when the TiO_2 respectively increased from 2% to 6% and 10% in the cement slurry. This reflects that the TiO_2 pigments have a beneficial effect on magnifying the white color of the hardened material, which aesthetically can be attractive in urban cities (besides its benefits on maintaining better air quality, as will be discussed later in the text) [31,33,34].

4.3. Effect on Mechanical Properties

As summarized in Table 1, the mechanical properties including f′c, fr, and pull-off bond followed an increasing trend with TiO_2 additions. For example, the f′c increased from 46.2 MPa for the control mix to 49 and 55.2 MPa when the slurry contained 4% and 8% TiO_2, respectively. The corresponding fr varied from 7.4 to 8.8 and 10.5 MPa, respectively, while the bond varied from 2.35 to 3.02 and 3.63 MPa, respectively. Such an increase in mechanical properties can be attributed to two phenomena, with the first one relating to the micro-filler as a result of the cement replacement by the finer TiO_2 particles. This phenomenon improves the matrix compacity and densifies its microstructure, leading to enhanced strengths. Besides the micro-filler effect, many researchers ascribed the increased strengths with TiO_2 additions to the formation of nucleation sites that promote the cement hydration reactions [29,31,45]. It is to be noted that the fracture failures for the tested bond specimens occurred mainly at the slurry/concrete interfaces, suggesting that this is the weakest plane in the system.

Figure 6 plots the variations in mechanical properties (i.e., Δ(f′c, fr, and Bond)) due to TiO_2 normalized with respect to the control mix. As shown, the Δ(f′c) gradually increased with 2% and 4% TiO_2 addition rates, which then tended to stabilize at about 18% ± 3% after a rate of 6%. This suggests that the optimum TiO_2 dosage on the strength development of cement slurries tested under compressive loading is about 6%. In contrast, it is interesting to note that the Δ(fr) and Δ(Bond) responses continued increasing up to 10% TiO_2 rates, suggesting that the tensile properties are positively affected regardless of the pigment rates. Hence, the Δ(fr) and Δ(Bond) reached, respectively, 45% and 61% at the TiO_2 rate of 10%. This phenomenon can be mainly attributed to the micro-filler effect that refines the pore structure, especially knowing that the tensile properties are highly influenced by the initiation and propagation of cracks [46,47]. Figure 7 illustrates the relationships between the 28-day f′c with respect to the fr and pull-off bond properties for the tested slurries; as shown, adequate relationships with correlation coefficients (R^2) higher than 0.91 can be established.

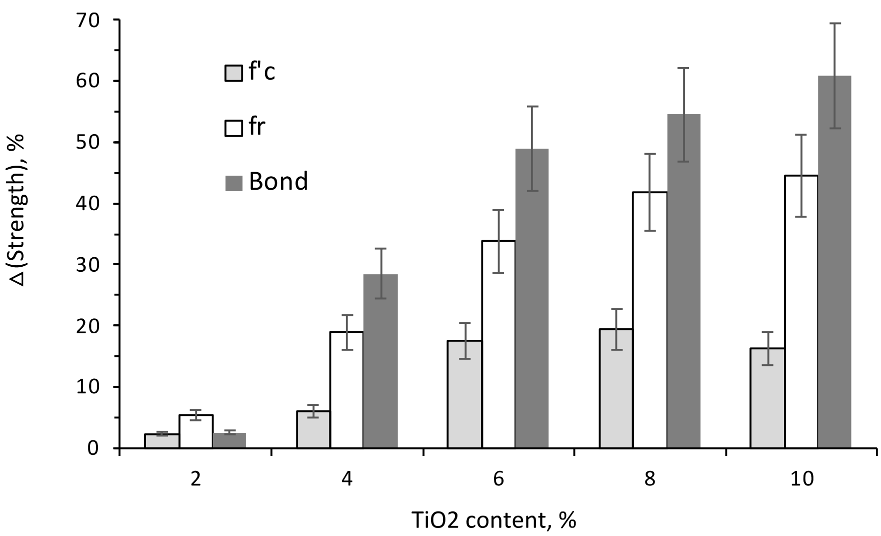

Figure 6. Effect of TiO_2 additions on Δ(f′c, fr, and Bond) values.

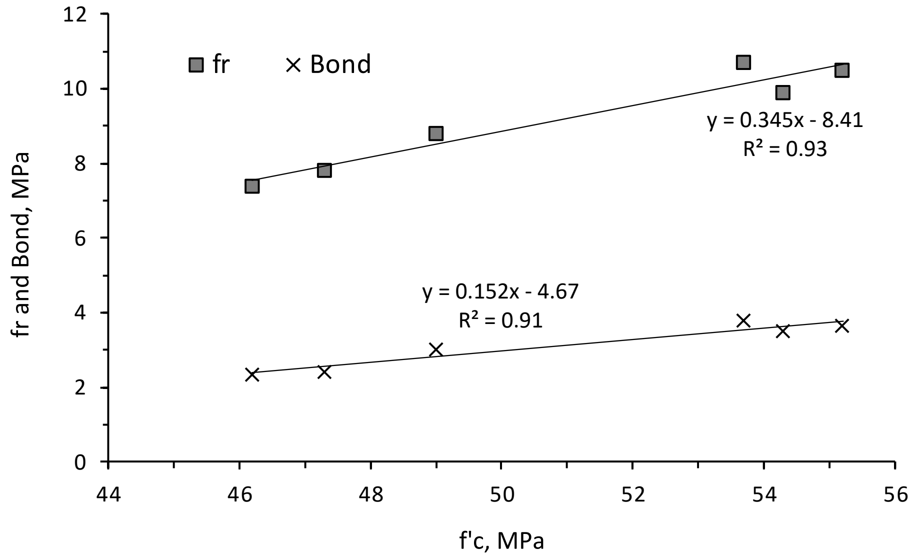

Figure 7. Relationships between f′c vs. fr and pull-off bond properties.

4.4. Effect on Water Absorption

Figure 8 illustrates some typical plots showing the variations of water absorption (in mm) over testing time (in square root of minutes) for the control mixture and those containing 4% and 8% TiO_2. The sorptivity (W_{abs}, mm/min$^{0.5}$) is computed as the slope of the resulting regression straight line; the R^2 values are higher than 0.99, reflecting that water absorption increases almost linearly at a constant rate over time.

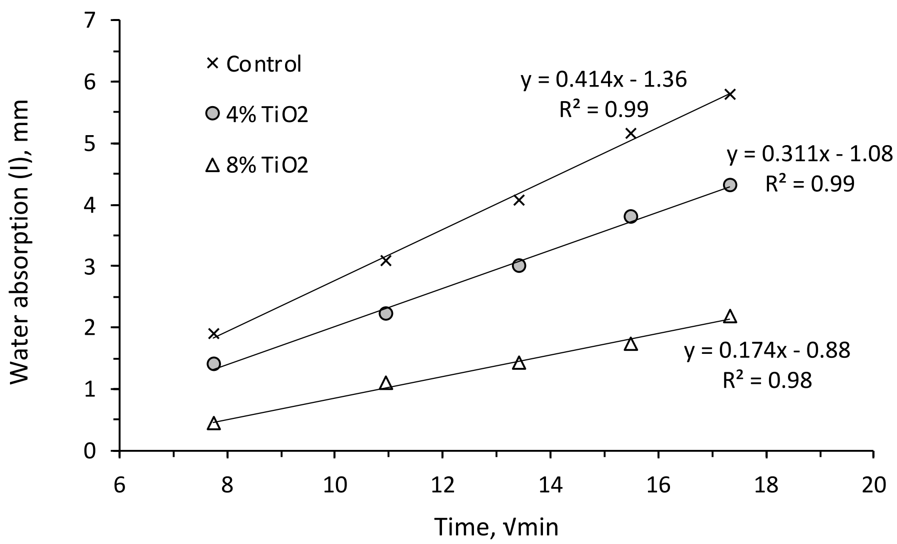

Figure 8. Typical variations in water absorption over time for selected slurries.

As shown in Figure 8 and summarized in Table 1, the W_{abs} dropped from 0.414 mm/min$^{0.5}$ for the control mix to 0.311 and 0.174 mm/min$^{0.5}$ for those containing TiO_2 additions. Such results are in agreement with the strength responses discussed earlier, revealing that the incorporation of pigments has beneficial effects on the hardened properties including the rate of water absorption. Hence, because of the micro-filler and nucleation effects, the compacity of the cement slurry improves, leading to reduced capillary pores that hinders the ease of water absorption over time [44]. It is to be noted that a good correlation exists between the f′c and W_{abs} responses, expressed in Equation (3) as:

$$W_{abs}, \text{mm/min}^{0.5} = -0.0225\ (f'c, \text{MPa}) + 1.439 \qquad (R^2 = 0.94) \tag{3}$$

The effect of TiO_2 on variations in $\Delta(W_{abs})$ values normalized with respect to the control mix is given in Figure 9. As shown, the $\Delta(W_{abs})$ gradually decreased to reach −9.6%, −25%, and −58% when the TiO_2 concentration increased to 2%, 4%, and 8%, respectively. This reflects the benefits of such additions to minimize the rate of water absorption, which can be particularly relevant to protect the external facades and surfaces for moisture-related problems (in addition to the photocatalytic activity that enhances the NOx removal). The $\Delta(W_{abs})$ slightly decreased to –43% at a TiO_2 rate of 10%, which may be attributed to an excess of fines that deteriorates the refinement of the pore structure.

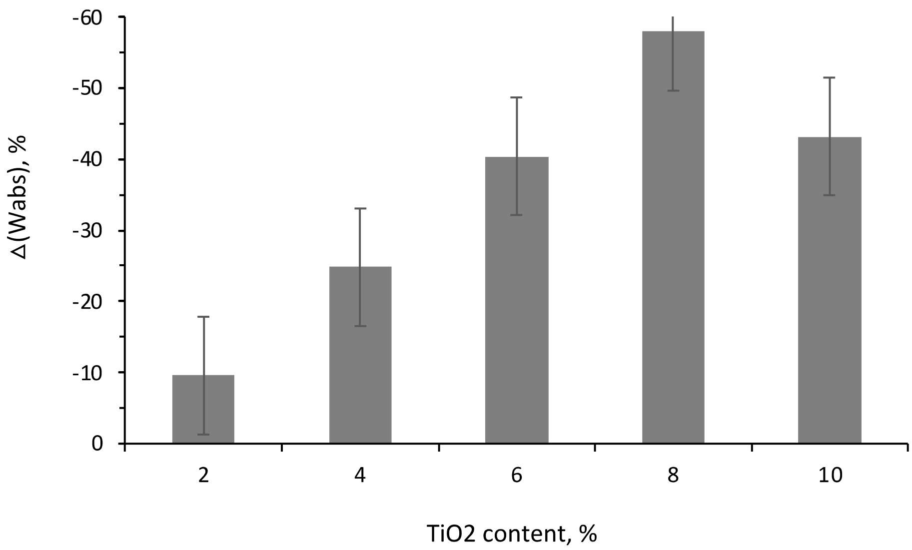

Figure 9. Effect of TiO_2 additions on $\Delta(W_{abs})$ values.

4.5. Effect on NOx Removal

Figure 10 shows the changes in NOx concentration as function of UV irradiation time for cement pastes prepared with various TiO_2 concentrations (i.e., 2.5%, 5%, and 10%) and different cement slurry thicknesses (i.e., 1 or 3 mm). Before irradiation, the NOx concentration in the reactor was 20 ppm. After about 5 min of light irradiation, the NOx concentration at the reactor outlet starts decreasing due to photocatalytic activities resulting from the incorporation of TiO_2, until reaching a steady state after about 25 to 45 min.

Figure 10 shows a significant increase in the removal efficiency with the increase in TiO_2 concentration. Hence, for instance, the NOx concentration at the reactor outlet dropped from 20 ppm for the control mix to 12 and 2 ppm with the incorporation of 2.5% and 5% TiO_2, respectively. Nevertheless, the mixture containing 10% TiO_2 appears to be less efficient in terms of photocatalytic efficiency, as compared to the mix prepared with 5% TiO_2. This can be attributed to a densification process of the slurry microstructure due to the higher TiO_2 concentration. Indeed, it is well known that the photocatalytic activity of TiO_2 embedded in cement-based materials depends on the microstructure porosity [48]. The decrease in porosity can reduce the adsorption capacity for pollutants and the full occurrence of the photocatalytic efficiency. The microstructure densification due to micro-filler and nucleation site effects of TiO_2 in cement-based materials is described in the literature [1,15]. Jiang et al. (2023) reported a 35% total porosity reduction when a high TiO_2 concentration is used [49–51]. In this present study, the results show an optimum of 5% TiO_2 beyond which the densification of the microstructure would prevent the complete penetration of NOx to the slurry and reduce the removal efficiency. This result is consistent with the water absorption results presented in Section 4.4, revealing that the thickness of the layer has no effect on the product efficiency.

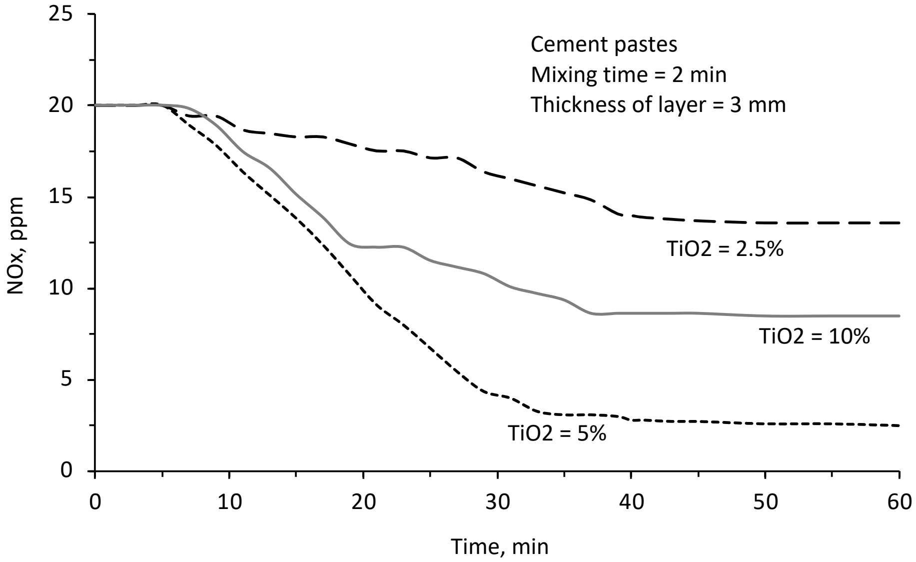

(**a**)

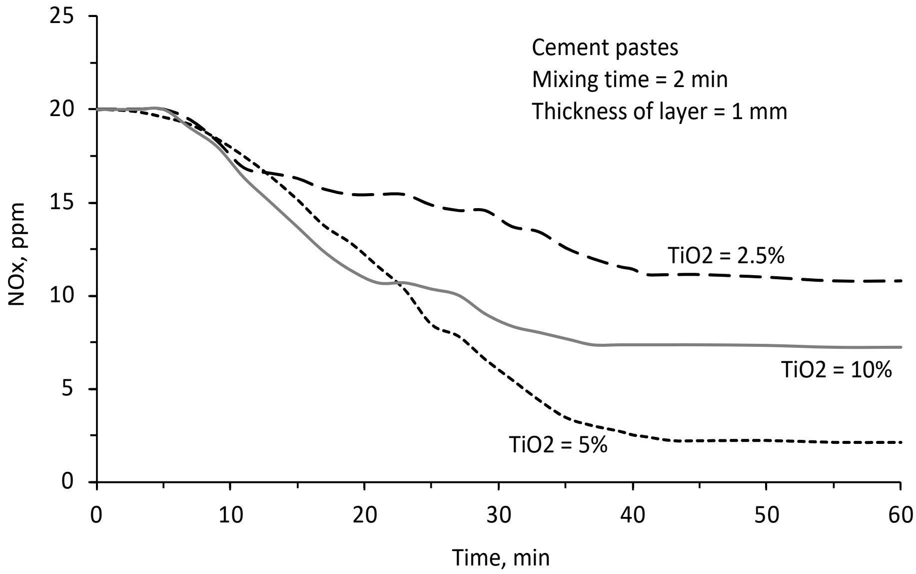

(**b**)

Figure 10. Variations of NOx concentrations at reactor outlet as a function of time for 3 mm (**a**) and 1 mm (**b**) cement slurry thicknesses.

The NOx removal percentage for various cement slurries prepared with different TiO_2 concentrations and applied on two coating thicknesses is illustrated in Figure 11 (dispersion time is fixed for 2 min). Clearly, the NOx removal is more affected by the TiO_2 content than by the slurry thickness. Indeed, independently of the thickness of the layer (1 or 3 mm), the 5% TiO_2 content appears to be the optimum concentration that exhibits the best NOx removal. On average, the NOx removal is about 39% for slurries containing 2.5% TiO_2, and 88% for the slurries containing 5% TiO_2, and then hovers about 60% for the ones containing 10% TiO_2. Practically, this reflects that the coating thickness has a limited effect on the photocatalytic activity, which can be economically advantageous in new construction or renovation applications.

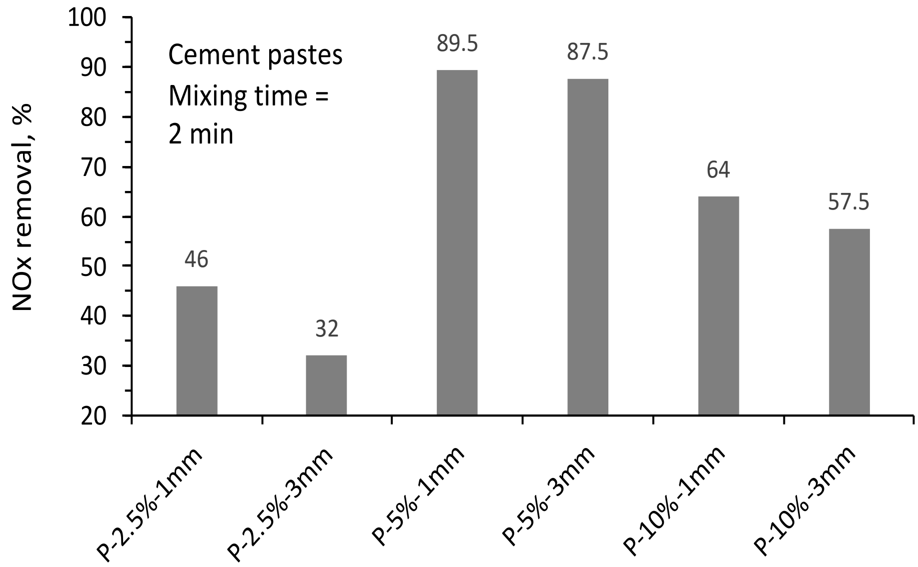

Figure 11. NOx removal (photocatalytic activity) for various TiO_2 concentrations of 2.5%, 5%, and 10% and two coating thickness (i.e., 1 and 3 mm).

The NOx removal percentage for various TiO_2 concentrations and two dispersion durations is shown in Figure 12. The results show no difference between a dispersion of 2 or 8 min, suggesting that the NOx removal is more affected by the TiO_2 content than by the dispersion time. Thus, two minutes of dispersion are sufficient to secure a maximum photocatalytic activity.

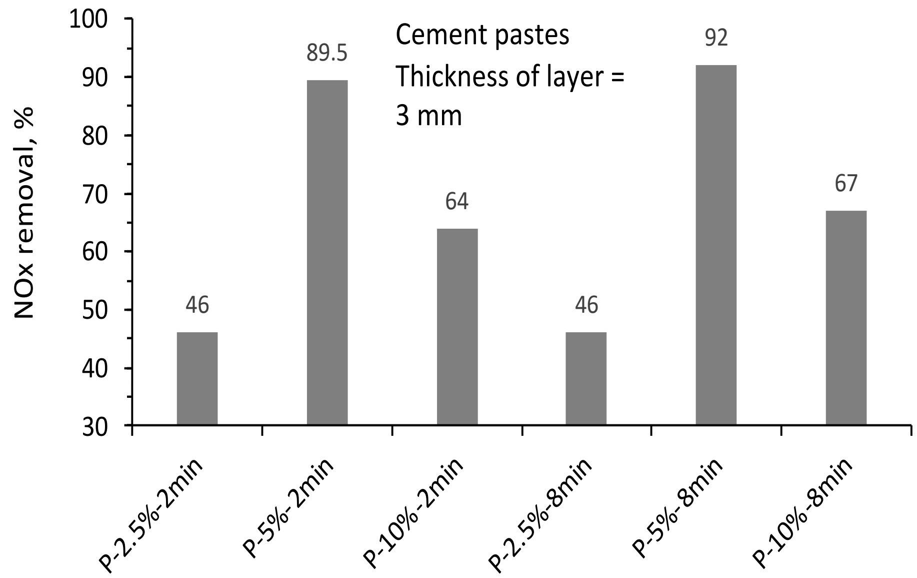

Figure 12. NOx removal (photocatalytic activity) for various TiO_2 concentrations of 2.5%, 5%, and 10% and two dispersion durations (i.e., 2 and 8 min).

5. Conclusions

Limited investigations assessed the efficiency of TiO_2-modified cement slurries to purify and abate ambient air pollutants. This study evaluates the influence of TiO_2 concentration, dispersion time during batching, and thickness on top of existing mortar blocks on photocatalytic activity using a reactor developed as per the ISO 22197-1:2007 specification. The validation of the test results using large-scale photocatalytic mock-ups are presented in a follow-up paper. Based on foregoing, the following conclusions can be warranted:

- The flow is marginally affected when up to 4% TiO_2 is added to the cement slurry, which thereafter gradually curtailed at higher rates. This was attributed to the fine TiO_2 particles that are believed to increase the inter-particle links within the suspension.
- The $\Delta(E)$ values gradually increased with the TiO_2 additions, reflecting their beneficial effects on magnifying the white color of the hardened material. This aesthetically can be attractive in urban cities, besides the associated benefits on maintaining better air quality.
- The mechanical properties improved with the TiO_2 additions due to two concurrent phenomena including the micro-filler effect and formation of nucleation sites that promote the cement hydration reactions. The improvement in strength was particularly noticed in the flexural and pull-off bond strengths.
- The incorporation of TiO_2 reduced the tendency towards water absorption, which is consistent with the improvement in the mechanical properties. The reduced rate of water absorption can be relevant to protect the external facades and surfaces for moisture-related problems.
- The NOx concentration at the reactor outlet dropped from 20 ppm for the control mix to 12 and 2 ppm with the incorporation of 2.5% and 5% TiO_2, respectively, reflecting the efficiency of TiO_2 additions. Nevertheless, the increase in TiO_2 to 10% appears to reduce the photocatalytic efficiency due to a densification process of the slurry microstructure.
- The NOx removal is marginally affected by the dispersion time used for preparing the TiO_2-modified slurry mixture, and also by the thickness of the slurry that is applied on the substrate surface. This can be economically advantageous in new construction or renovation applications.
- The cement slurry containing 5% TiO_2, mixed for 2 min, and applied at a 1 mm thickness exhibited the highest photocatalytic efficiency. This can be recommended for cement slurries used in the construction industry, either in new structures or for the renovation of existing facades.

Author Contributions: Funding acquisition, J.A. and Y.J.; investigation, Y.J.; methodology, J.A. and Y.J.; project administration, J.A. and Y.J.; resources, J.A., Y.J. and G.A.; supervision, J.A. and Y.J.; validation, J.A., Y.J. and G.A.; visualization, J.A., Y.J. and G.A.; writing—original draft, Y.J.; writing—review and editing, J.A., Y.J. and G.A. All authors have read and agreed to the published version of the manuscript.

Funding: This research received no external funding.

Data Availability Statement: The data presented in this study are available on request from the corresponding author.

Conflicts of Interest: The authors declare no conflict of interest.

References

1. Chen, J.; Poon, C.-S. Photocatalytic Cementitious Materials: Influence of the Microstructure of Cement Paste on Photocatalytic Pollution Degradation. *Environ. Sci. Technol.* **2009**, *43*, 8948–8952. [CrossRef]
2. Duncan, B.N.; Lamsal, L.N.; Thompson, A.M.; Yoshida, Y.; Lu, Z.; Streets, D.G.; Hurwitz, M.M.; Pickering, K.E. A space-based, high-resolution view of notable changes in urban NOx pollution around the world (2005–2014). *J. Geophys. Res. Atmos.* **2016**, *121*, 976–996. [CrossRef]
3. Anderegg, W.R.L.; Prall, J.W.; Harold, J.; Schneider, S.H. Expert credibility in climate change. *Proc. Natl. Acad. Sci. USA* **2010**, *107*, 12107–12109. [CrossRef] [PubMed]
4. Sikkema, J.; Ong, S.; Alleman, J. Photocatalytic concrete pavements: Laboratory investigation of NO oxidation rate under varied environmental conditions. *Constr. Build. Mater.* **2015**, *100*, 305–314. [CrossRef]
5. WHO. Air Quality Guidelines—Global Update. 2005. Available online: https://www.who.int/phe/health_topics/outdoorair/outdoorair_aqg/en/ (accessed on 11 October 2011).
6. Pérez-Nicolás, M.; Plank, J.; Ruiz-Izuriaga, D.; Navarro-Blasco, I.; Fernández, J.; Alvarez, J. Photocatalytically active coatings for cement and air lime mortars: Enhancement of the activity by incorporation of superplasticizers. *Constr. Build. Mater.* **2018**, *162*, 628–648. [CrossRef]
7. Hassan, M.M.; Dylla, H.; Mohammad, L.N.; Rupnow, T. Evaluation of the durability of titanium dioxide photocatalyst coating for concrete pavement. *Constr. Build. Mater.* **2010**, *24*, 1456–1461. [CrossRef]

8. Wu, X. Applications of titanium dioxide materials. In *Titanium Dioxide—Advances and Applications*; IntechOpen: London, UK, 2022. [CrossRef]
9. Cárdenas, C.; Tobón, J.I.; García, C.; Vila, J. Functionalized building materials: Photocatalytic abatement of NOx by cement pastes blended with TiO_2 nanoparticles. *Constr. Build. Mater.* **2012**, *36*, 820–825. [CrossRef]
10. Lee, B.Y.; Jayapalan, A.R.; Bergin, M.H.; Kurtis, K.E. Photocatalytic cement exposed to nitrogen oxides: Effect of oxidation and binding. *Cem. Concr. Res.* **2014**, *60*, 30–36. [CrossRef]
11. Saleh, H.M.; El-Sheikh, S.M.; Elshereafy, E.E.; Essa, A.K. Mechanical and physical characterization of cement reinforced by iron slag and titanate nanofibers to produce advanced containment for radioactive waste. *Constr. Build. Mater.* **2019**, *200*, 135–145. [CrossRef]
12. Saleh, H.M.; Salman, A.A.; Faheim, A.A.; El-Sayed, A.M. Influence of aggressive environmental impacts on clean, lightweight bricks made from cement kiln dust and grated polystyrene. *Case Stud. Constr. Mater.* **2021**, *15*, e00759. [CrossRef]
13. Ramirez, A.M.; Demeestere, K.; Belie, N.D.; Mäntylä, T.; Levänen, E. Titanium dioxide coated cementitious materials for air purifying purposes: Preparation, characterization and toluene removal potential. *Build. Environ.* **2010**, *45*, 832–838. [CrossRef]
14. Delnavaz, M.; Ayati, B.; Ganjidoust, H.; Sanjabi, S. Application of concrete surfaces as novel substrate for immobilization of TiO_2 nano powder in photocatalytic treatment of phenolic water. *J. Environ. Health Sci. Eng.* **2015**, *13*, 58. [CrossRef]
15. Yang, J.; Wang, G.; Wang, D.; Liu, C.; Zhang, Z. A self-cleaning coating material of TiO_2 porous microspheres/cement composite with high-efficient photocatalytic depollution performance. *Mater. Lett.* **2017**, *200*, 1–5. [CrossRef]
16. Li, Q.; Liu, Q.; Peng, B.; Chai, L.; Liu, H. Self-cleaning performance of TiO_2 -coating cement materials prepared based on solidification/stabilization of electrolytic manganese residue. *Constr. Build. Mater.* **2016**, *106*, 236–242. [CrossRef]
17. *ISO 22197-1:2007*; Fine Ceramics (Advanced Ceramics, Advanced Technical Ceramics). Test Method for Air-Purification Performance of Semiconducting Photocatalytic Materials. ISO: London, UK, 2007. [CrossRef]
18. *JSA-JIS R1701-1*; Fine Ceramics (Advanced Ceramics, Advanced Technical Ceramics)—Test Method for Air Purification Performance of Photocatalytic Materials—Part 1: Removal of Nitric Oxide. Japanese Standards Association: Tokyo, Japan, 2016.
19. Jimenez-Relinque, E.; Rodriguez-Garcia, J.; Castillo, A.; Castellote, M. Characteristics and efficiency of photocatalytic cementitious materials: Type of binder, roughness and microstructure. *Cem. Concr. Res.* **2015**, *71*, 124–131. [CrossRef]
20. Li, Z.; Ding, S.; Yu, X.; Han, B.; Ou, J. Multifunctional cementitious composites modified with nano titanium dioxide: A review. *Compos. Part A Appl. Sci. Manuf.* **2018**, *111*, 115–137. [CrossRef]
21. Binas, V.; Papadaki, D.; Maggos, T.; Katsanaki, A.; Kiriakidis, G. Study of innovative photocatalytic cement based coatings: The effect of supporting materials. *Constr. Build. Mater.* **2018**, *168*, 923–930. [CrossRef]
22. Witkowski, H.; Jackiewicz-Rek, W.; Chilmon, K.; Jarosławski, J.; Tryfon-Bojarska, A.; Gąsiński, A. Air Purification Performance of Photocatalytic Concrete Paving Blocks after Seven Years of Service. *Appl. Sci.* **2019**, *9*, 1735. [CrossRef]
23. Martinez, T.; Bertron, A.; Ringot, E.; Escadeillas, G. Degradation of NO using photocatalytic coatings applied to different substrates. *Build. Environ.* **2011**, *46*, 1808–1816. [CrossRef]
24. Daniyal, M.; Akhtar, S.; Azam, A. Effect of nano-TiO_2 on the properties of cementitious composites under different exposure environments. *J. Mater. Res. Technol.* **2019**, *8*, 6158–6172. [CrossRef]
25. Lee, J.W.; Lee, S.H.; Jang, Y.I.; Park, H.M. Evaluation of reducing no and SO_2 concentration in nano SiO_2-TiO_2 photocatalytic concrete blocks. *Materials* **2021**, *14*, 7182. [CrossRef] [PubMed]
26. Lapidus, A.; Korolev, E.; Topchiy, D.; Kuzmina, T.; Shekhovtsova, S.; Shestakov, N. Self-cleaning cement-based building materials. *Buildings* **2022**, *12*, 606. [CrossRef]
27. Diamanti, M.V.; Luongo, N.; Massari, S.; Lupica Spagnolo, S.; Daniotti, B.; Pedeferri, M.P. Durability of self-cleaning cement-based materials. *Constr. Build. Mater.* **2021**, *280*, 122442. [CrossRef]
28. Jimenez-Relinque, E.; Castellote, M. Quick assessment of the photocatalytic activity of TiO_2 construction materials by nitroblue tetrazolium (NBT) ink. *Constr. Build. Mater.* **2019**, *214*, 1–8. [CrossRef]
29. Folli, A.; Pade, C.; Hansen, T.B.; De Marco, T.; Macphee, D.E. TiO_2 photocatalysis in cementitious systems: Insights into self-cleaning and depollution chemistry. *Cem. Concr. Res.* **2012**, *42*, 539–548. [CrossRef]
30. Assaad, J.J. Disposing waste latex paints in cement based materials—Effect on flow and rheological properties. *J. Build. Eng.* **2016**, *6*, 75–85. [CrossRef]
31. Assaad, J.J.; Nasr, D.; Chwaifaty, S.; Tawk, T. Parametric study on polymer-modified pigmented cementitious overlays for colored applications. *J. Build. Eng.* **2020**, *27*, 101009. [CrossRef]
32. Bartos, P. *Fresh Concrete Properties and Test*; Elsevier: Amsterdam, The Netherlands, 1992; ISBN 0444881417.
33. Yildizel, S.A.; Kaplan, G.; Ozturk, A.U. Cost optimization of mortars containing different pigments and their freeze-thaw resistance properties. *Adv. Mater. Sci. Eng.* **2016**, *2016*, 5346213. [CrossRef]
34. Hospodarova, V.; Junak, J.; Stevulova, N. Color pigments in concrete and their properties. *Pollack Period.* **2015**, *10*, 143–151. [CrossRef]
35. Assaad, J.J. Effect of Waste Latex Paint on Rheological Properties of Cement Pastes—Compatibility with Water Reducers. *Jr. Mater. Civ. Eng.* **2015**, *27*, 12. [CrossRef]
36. Buxbaum, G. *Industrial Inorganic Pigments*, 2nd ed.; WILEY-VCH: Weinheim, Germany, 1998.
37. Teichmann, G. The use of colorimetric methods in the concrete industry. *Betonw. Fertigtl.* **1990**, *11*, 58–73.
38. *BS EN 196/1*; Methods of Testing Cement. Determination of Strength. British Standard Institution: London, UK, 2016; p. 38.

39. *EN 1542*; Products and Systems for the Protection and Repair of Concrete Structures. Test Methods. Measurement of Bond Strength by Pull-Off. BSI: London, UK, 1999.
40. Issa, C.; Assaad, J. Stability and Bond Properties of Polymer-Modified Self-Consolidating Concrete for Repair Applications. *Mater. Struct.* **2017**, *50*, 28. [CrossRef]
41. Assaad, J.J. Development of Polymer-Modified Cement for Adhesive and Repair Applications. *Constr. Build. Mater.* **2018**, *163*, 139–148. [CrossRef]
42. *ASTM C1585-13*; Standard Test Method for Measurement of Rate of Absorption of Water by Hydraulic-Cement Concretes. ASTM International: West Conshohocken, PA, USA, 2013.
43. Assaad, J.; Issa, C. Use of Locked-Cycle Protocol to Assess Cement Fineness and Properties in Laboratory-Grinding Mills. *ACI Mater. J.* **2016**, *113*, 429–438. [CrossRef]
44. Wang, D.; Shi, C.; Farzadnia, N.; Shi, Z.; Jia, H. A review on effects of limestone powder on the properties of concrete. *Constr. Build. Mater.* **2018**, *192*, 153–166. [CrossRef]
45. Nazari, A.; Riahi, S. The effect of TiO_2 nanoparticles on water permeability and thermal and mechanical properties of high strength self-compacting concrete. *Mater. Sci. Eng. A* **2010**, *528*, 756–763. [CrossRef]
46. Beushausen, H.; Gillmer, M. The use of superabsorbent polymers to reduce cracking of bonded mortar overlays. *Cement Concr. Compos.* **2014**, *52*, 1–8. [CrossRef]
47. El Sakka, F.; Assaad, J.J.; Hamzeh, F.; Nakhoul, C. Thixotropy and interfacial bond strengths of polymer-modified printed mortars. *Mater. Struct.* **2019**, *52*, 79. [CrossRef]
48. Zhang, J.; Tan, H.; Deng, X. NOx removal ability of photocatalytic cement-based materials with porous structure. *J. Clean. Prod.* **2022**, *377*, 134396. [CrossRef]
49. Jiang, J.; Dong, X.; Wang, H.; Wang, F.; Li, Y.; Lu, Z. Enhanced mechanical and photocatalytic performance of cement mortar reinforced by nano-TiO_2 hydrosol-coated sand. *Cem. Concr. Compos.* **2023**, *137*, 104906. [CrossRef]
50. Saade, J.; Assaad, J.J. Effect of Pigments on Structural Properties of Colored Reinforced Concrete Beams. *Adv. Civ. Eng. Mater.* **2022**, *11*, 17–32. [CrossRef]
51. Assaad, J.J.; Mattew, M.; Saade, J. Effect of Pigments on Bond Strength Between Coloured Concrete and Steel Reinforcement. *Acta Polytech.* **2022**, *62*, 248–261. [CrossRef]